AALBORG UNIVERSITY
DENMARK

Development of a wireless crank moment measurement-system for a handbike: Initial results of propulsion kinetics

Lasse Jakobsen[1] *& Frederik Husted Ahlers*[2]

Abstract

Objective: Develop a wireless crank moment measurement system for a handbike. **Method:** A tee-rosette strain gage was mounted on the crankshaft and connected to a wireless transmitter. An optical wheel encoder provided crank position and speed data in order to determine applied crank force with respect to position and calculation of power. **Results:** Linearity (R^2=1) was demonstrated between applied force and voltage output for 1,2,3,4 and 5 kg load for the calibration procedure. The initial propulsion measurement presented data for applied crank moment, tangential force, angular velocity and power with respect to crank position. **Discussion:** This system can provide kinetic data in terms of tangential external force, provided by the athlete and as input for biomechanical modelling. This system has the potential to obtain field measurement on the road, due to the wireless system.

Keywords: Handbike, hand cycling, propulsion force, strain gage

Introduction:

Pedal force measurements are common in the scientific research field of cycling. The information of the force magnitude and direction on the pedals can be analyzed and force production effectiveness can be identified. (Bini & Carpes 2014). This would also be applicable for optimizing hand cycling propulsion effectiveness, though it is rarely seen (Arnet 2012b). For people with lower limb impairments, hand cycling as a sport activity has become popular since it was implemented in the Paralympic Games in 2004 (Faupin & Gorce 2008). Thus, the interest in relation to performance optimization has likewise arisen in the field of hand cycling, where the handbike interface has been under investigation (Arnet 2012b, Faupin & Gorce 2008, Goosey-Tolfrey, et al. 2008, Litzenberger et al. 2015). Depending on the specific research scope, propulsion force measurements can be used for analysis of performance. Additionally, propulsion force measurement can provide input for biomechanical models. A wide range of commercially available power sensors already exist on the market such as the SRM power meter, Quarq power meter and Garmin Vector power meter (Garmin , SRM , Quarq). Common for all systems is an average measure of power output for a number of complete revolutions. Hence, these systems do not provide detailed force information for a single propulsion cycle. Detailed force measurements in the scientific research field of hand cycling, is however determined in various ways and varies in accuracy and detail as well (Arnet 2012b, Bafghi et al. 2008, Verellen et al. 2004). The system developed by Arnet (2012a) implied an FS6-500 force sensor (AMTI,

[1] l*asse@stagsted.net* - M.Sc Stud. Aalborg University
[2] *frehust@gmail.com* - M.Sc Stud. Aalborg University

Crowthorne, England), measuring forces in three directions and therefore provided a detailed force measurement. With this system, Arnet (2012a) found that the tangential force during the hand cycling propulsion was the most dominant (Arnet 2012a). However, the FS6-500 is an expensive and wire based sensor, thus a large and heavy wire must follow the handbike handle during the propulsion and are unsuitable for force measuring on the road. This leads to the aim of this technical note, which was to provide technical information on a wireless and relatively inexpensive crank moment measurement system and to document its accuracy.

Method and materials

The procedure of this technical note consisted of two main steps.

1. Develop a system able to measure moment applied to the crankshaft during hand cycling propulsion.
2. Collect initial propulsion measurement data for crank moment applied to the crankshaft over the propulsion cycle.

1. System design

The system must meet the following overall requirements:

- Force measurement of the tangential force applied to the crankshaft for each revolution, during hand cycling.
- Determination of crank position and angular velocity.
- Synchronize force and crank position data, in order to locate force with respect to crank position and calculate power.

The system design was subdivided into “force measurement”, “calibration”, “crank position measurement” and “force and position synchronization”, in order to acquire the three requirements stated above. For “force measurement”, “crank position measurement” and “force and position synchronization” a set of requirements for each subpart was determined, in order to ensure acceptable data quality.

Force measurement

The force measurement part of the system must meet the following requirements:

- Measure crankshaft moment and thereby tangential force applied to the pedals, during the hand cycling propulsion movement.
- Sample at least 20 HZ in order to detect the changes in force for one propulsion cycle. The minimum sampling rate is based on the force measurement characteristics when propelling a

handbike with 60-70 rmp, obtained by Arnet et al (2012a) and accounts for Nyquist minimal sampling rate.

- Sample wireless in order to avoid entangling wires, during hand cycling propulsion.

When force is applied to the pedal, the crankshaft is submitted to torsion. During torsion, the principal normal stresses occur at an angle of ±45° with respect to the longitudinal axis of the crankshaft (Hoffmann 1989a). Therefore, a CEA-XX-125UT-350 tee-rosette strain gage (Micro measurement, Wendell, USA) was mounted on the crankshaft surface between the two crank bearings at an angle of 45°, with respect to the longitudinal axis. The strain gage was mounted between the crank tooth wheel and the right handle. Thus, the measure for crank moment did only correspond to the force contribution from the right arm. The tee-rosette contains two strain gages oriented at 90° with respect to each other. The strain gage was setup as a Wheatstone half-bridge circuit (Hoffmann 1989b).

The tee-rosette strain gage was connected to a V-Link®-LXRS® Wireless 7 Channel analog input sensor node (LORD Corporation, Williston, USA), according to the node manual (LORD 2015). The node was mounted at the left crank arm, thus it rotated in sync with the strain gage during the propulsion cycle. Sample rate was set to 512 HZ with one sensor input channel enabled. The sensor analog data was digitized in the node and wirelessly transmitted to an WSDA®-Base-101 Analog Output Base Station (LORD, Corporation, Williston, USA), connected to a laptop running node commander 2.17.0 (LORD Corporation, Williston, USA). Simultaneously, the analog output from the base station was wire-connected to a NI USB-6008/6009DAQ USB Device (National Instruments, Texas, USA) as illustrated in figure 3.

Calibration

In order to determine the crank moment from the voltage output given from the strain gage, a calibration procedure was performed. Thus, a specific voltage output corresponded to a specific applied crank moment.

The crank was locked vertically in a vice, as close to the crank box as possible. The pedal arms were placed horizontal at 90° with respect to vertical and the crank tooth wheel was fixed in this position. A string was fastened on the right pedal arm and loaded with 1,2,3,4 and 5 kilograms respectively. For every load, the voltage output from the strain gage changed and was sampled for five seconds. The average of the five second samples represented a measuring point for each load condition. The setup is illustrated in figure 1. The procedure was repeated three times with three different gains ±1 mV(gain 1214), ±2.5 mV (569) and ±5 mV(gain 291). The calibration wizard in node commander was performed for all gains prior to applying loads (LORD 2015).

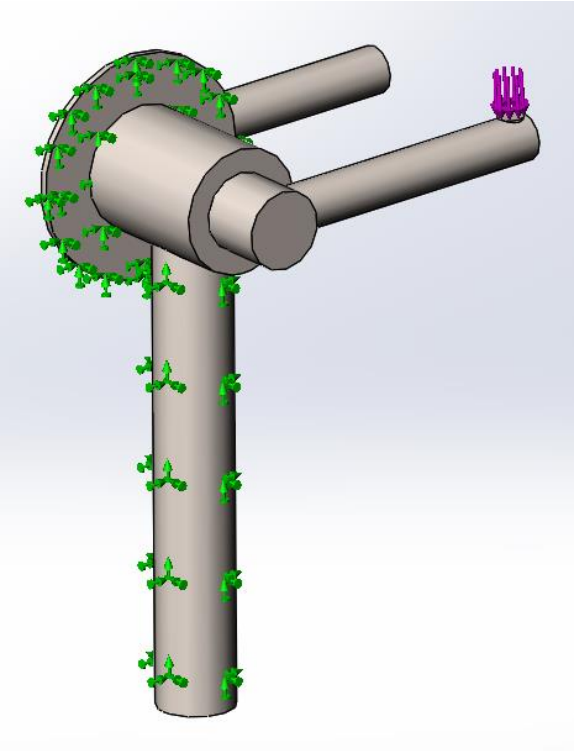

Figure 1: Calibration illustration (green arrows illustrates the fixed surfaces and the purple arrows represents applied force)

Crank position measurement

The part of the system determining the crank position must meet the following requirements:

- Determine crank position and angular velocity for each crank revolution.
- Be low frictional in order to minimize braking effect.

The position measurement must determine crank position with respect to applied moment. In addition, the position measurement must provide velocity data for power calculation (Watt). In this context, a HEDS-5540-A06 optical wheel encoder (Hewlett Packard, California, USA), with 500 impulses per revolution was used as the device for crank position determination. A tooth wheel was mounted on the crankshaft and connected to a second tooth wheel, mounted on a shaft entering the encoder. Hence, one revolution for the crankshaft corresponded to one revolution for the encoder and therefore 500 impulses. The CAD model of the crank position system is illustrated in figure 2.

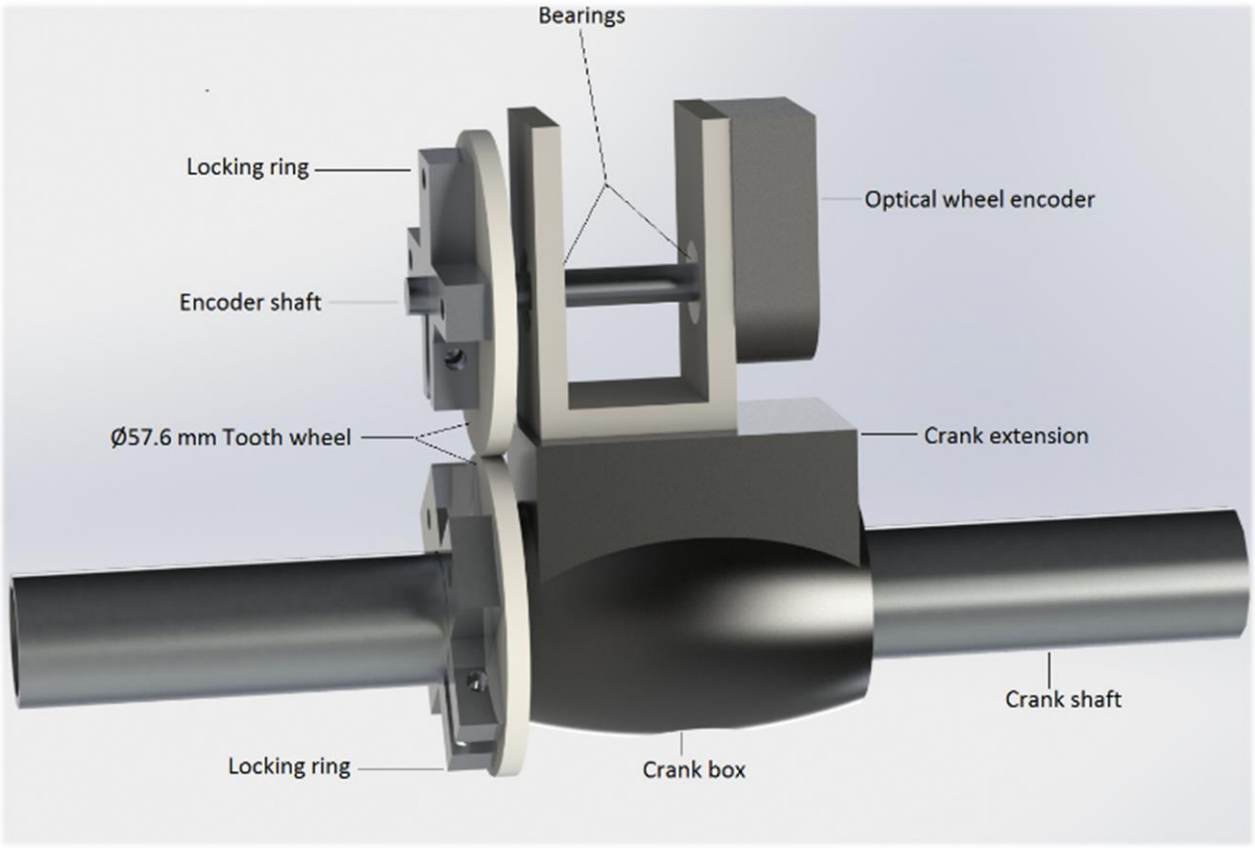

Figure 2: Crank position CAD model

The encoder contained an A channel and a 90°phase shifted B channel, enabling the ability to determine rotation direction. Like the WSDA®-Base-101 Analog Output Base Station, the encoder was also connected to the NI USB-6008/6009DAQ USB Device, where the analog encoder signal was digitized. The connection is presented in figure 3.

Force and position synchronizing

The force and position synchronizing subpart of the system must meet the following requirements:

- Sample at least same frequency as the wireless node connected to the strain gage, in order to avoid data loss.
- Position measurement and force measurement must be synchronized.

In order to determine the crank position with respect to the crank moment, the data were synchronized. As described previously, the force measurement and the position measurement subpart of the system, were connected to the NI USB-6008/6009DAQ USB Device. Thus, both signals were entering the same A/D converter simultaneously. A GUI (Graphical user interface) was set up in LabVIEW 2015 sp 1 (National Instruments, Texas, USA), with a live display for crank position and voltage given from the strain gage. The

GUI was set to start record, stop record and save the two signals simultaneously, resulting in two equal length data strings representing encoder counts and strain gage voltage. The NI USB-6008/6009DAQ USB Device sampled with 16000 HZ for each channel (two channels for the encoder and one channel for the strain gage). The force measurement and crank position measurement connection and synchronizing setup is illustrated in figure 3.

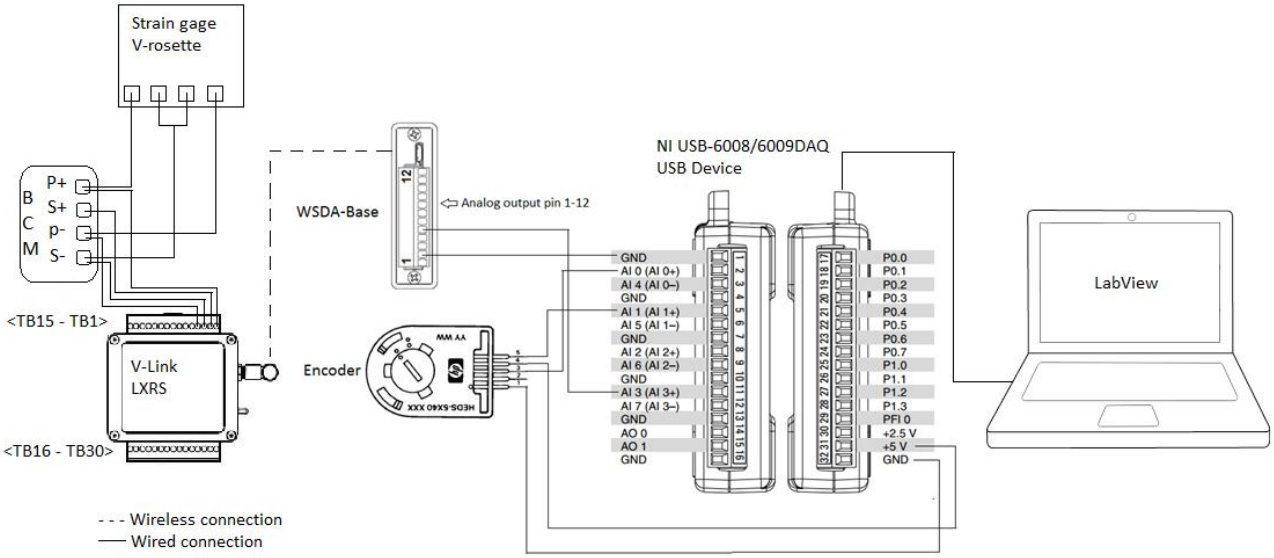

Figure 3 : Force and position synchronizing setup. The strain gage is wire connected to the V-Link wireless node via a bridge complete module (BCM) and transmits the digital signal wireless to the WSDA-Base station. The NI USB-6008/6009DAQ USB Device receives the strain signal along with the A and B channels from the encoder. Thus, the data are synchronized in the DAQ USB and then visualized in LabVIEW.

Wireless delay test

A delay test was performed in order to account for a possible delay related to the wireless signal transmission. The V-Link®-LXRS® Wireless 7 Channel analog input sensor node was supplied with a sine signal from a power supply. The sine signal was recorded with an oscilloscope from one output channel on the WSDA®-Base-101 Analog Output Base Station. Simultaneously, the power supply was wire connected to the oscilloscope. This enabled the ability to compare the wire and wireless signals and examining any possible delay.

2 Initial propulsion measurement

One able subject (age 26, mass 82 kilograms, height 1.8 m) participated in the initial propulsion measurement. The strain gage gain was calibrated to ±1 mV as described previously in section “calibration”. The subject propelled a handbike connected to a modified KICKR bicycle home trainer (Wahoo Fitness, Atlanta, USA), for 10 revolutions at a freely chosen speed. The crank was placed 370 mm vertically to the base plate of the handbike and 130 mm horizontal with respect to the vertical tube connected to the head

tube. The backrest was placed in an angle of 158° with respect to horizontal (see figure 4). At the crank start position, the pedals pointed vertically towards the ground. Resistance was controlled with the Bluetooth Powered Cycling and Running Workout Tracker 5.7.7 application (Wahoo Fitness, Atlanta, USA) and set to 35%.

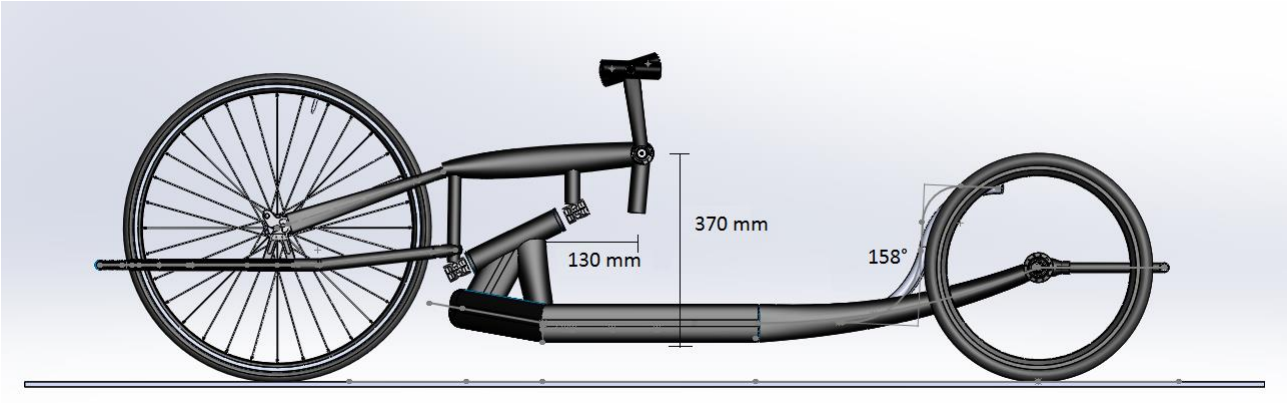

Figure 4 : Handbike setup. Measures of crank position (370 mm vertically to the base plate, 130 mm horizontal with respect to the vertical tube connected to the head tube and backrest angle of angle of 158°)

The subjects' anatomical location with respect to the crank is illustrated in figure 5, where it is evident that the shoulder and elbow joint is located below the crank.

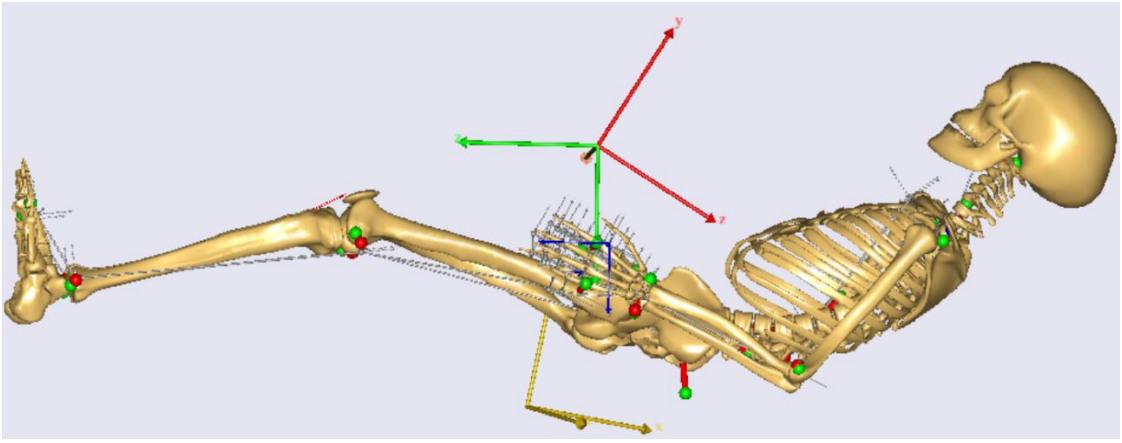

Figure 5 : The crankshaft is represented by the red and green coordinate system. The shoulder position is located below the crank and the power output, tangential force and crankshaft moment will reflects the position.

Data analysis

For the calibration, coefficient of determination (R^2) was calculated between voltage and applied force. The 500-encoder impulses, representing one crank cycle, were divided by 360° leading to 1.389 impulses per degree. The raw data for the initial propulsion measurement was filtered with a Butterworth 10 HZ low pass filter. Data processing was done in MatLab R2015b (MathWorks, Incorporation**,** Massachusetts, USA) and Excel 2013 (Microsoft, Washington, USA).

Results

Calibration: The results for the calibration procedure is illustrated in figure 6 and represent the correlation between the applied load and the voltage output for 1 mV, 2.5 mV and 5 mV gain. The correlation value R^2 was 1.0 for all three gains, thus representing a linear correlation.

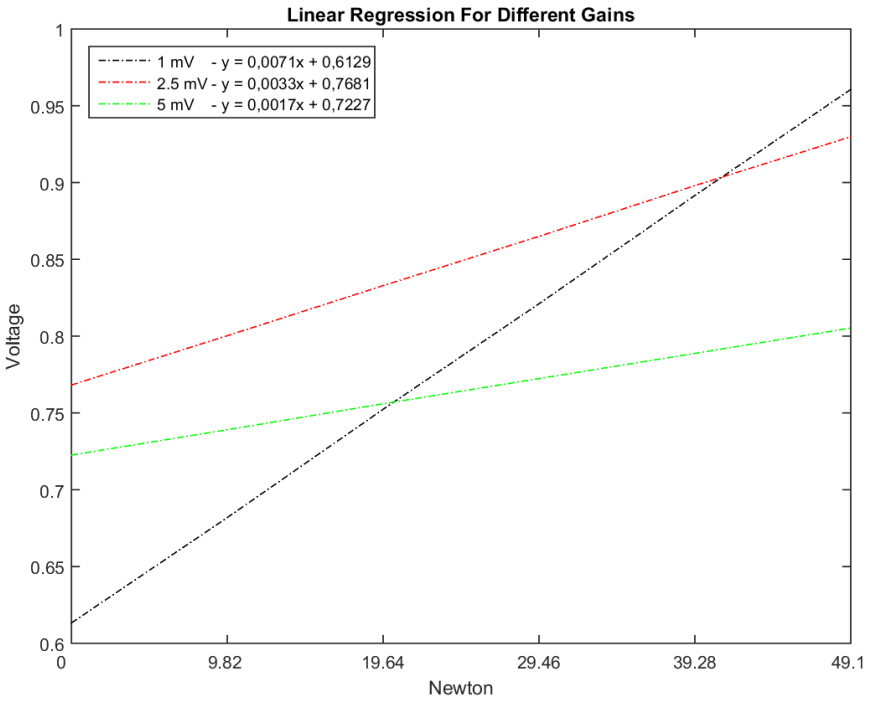

Figure 6 : Correlation between applied load and voltage output for calibration with 1 mV (blue), 2.5 mV (red) and 5 mV (green) gain. X-axis shows applied force in Newton and Y-axis shows output voltage.

Wireless delay test: The wireless delay test found a delay of 4 ms when converting and transmitting the signal from the V-Link®-LXRS® Wireless 7 Channel analog input sensor node to the WSDA®-Base-101 Analog Output Base Station.

Initial propulsion measurement: The force measurement results for the initial propulsion measurement are presented in figure 7-10. Figure 7 illustrates crank moment and tangential force as a mean ±SD for revolution six-nine. The individual ten revolutions representing crank moment and tangential force are presented in figure 8. The propulsion speed for all ten revolutions are illustrated in figure 9.

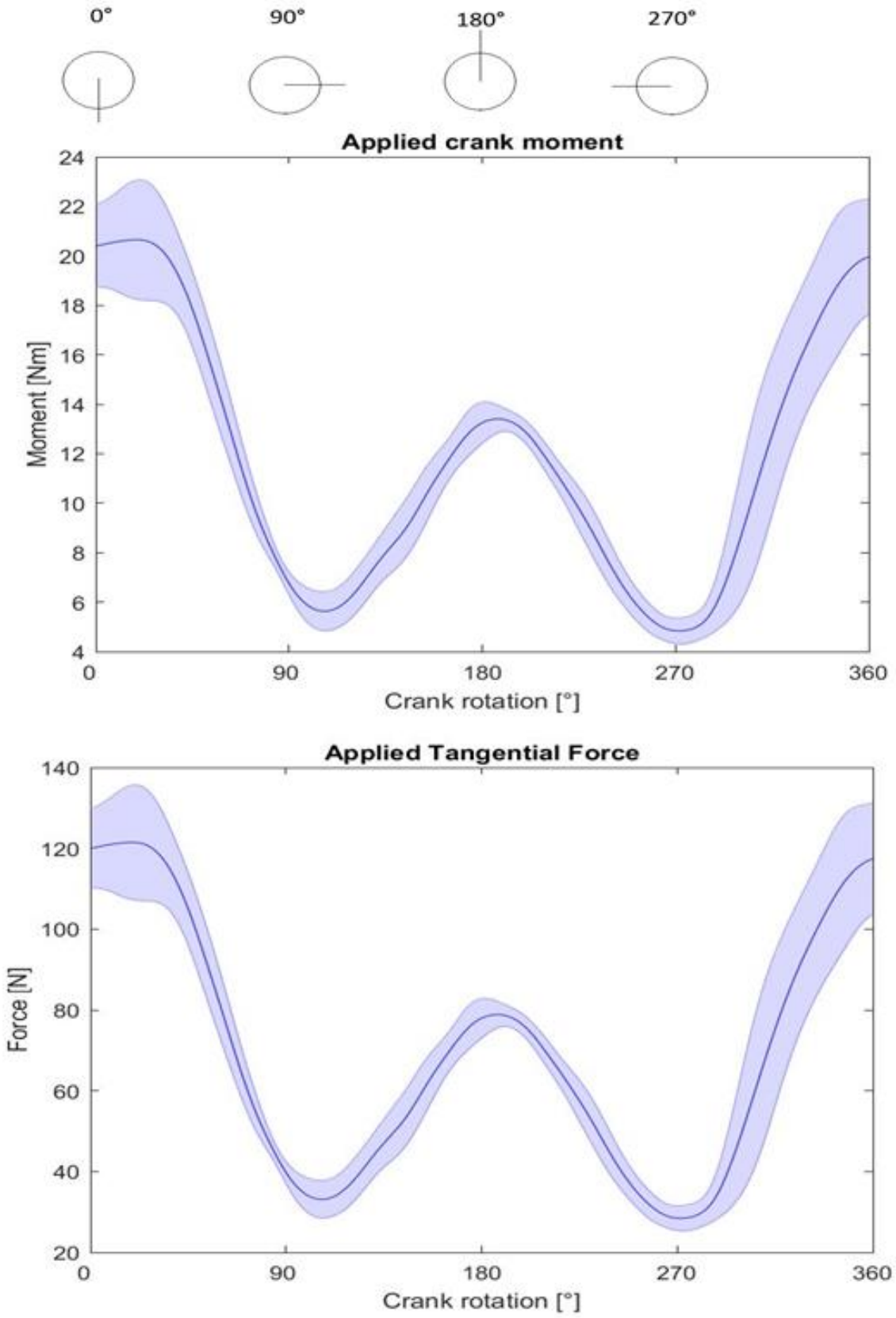

Figure 7 : Average crank moment and tangential force for revolution 6-9 ± SD, with respect to crank position (0-360°). 0° is represents the position when the pedals are pointing vertically towards the ground.

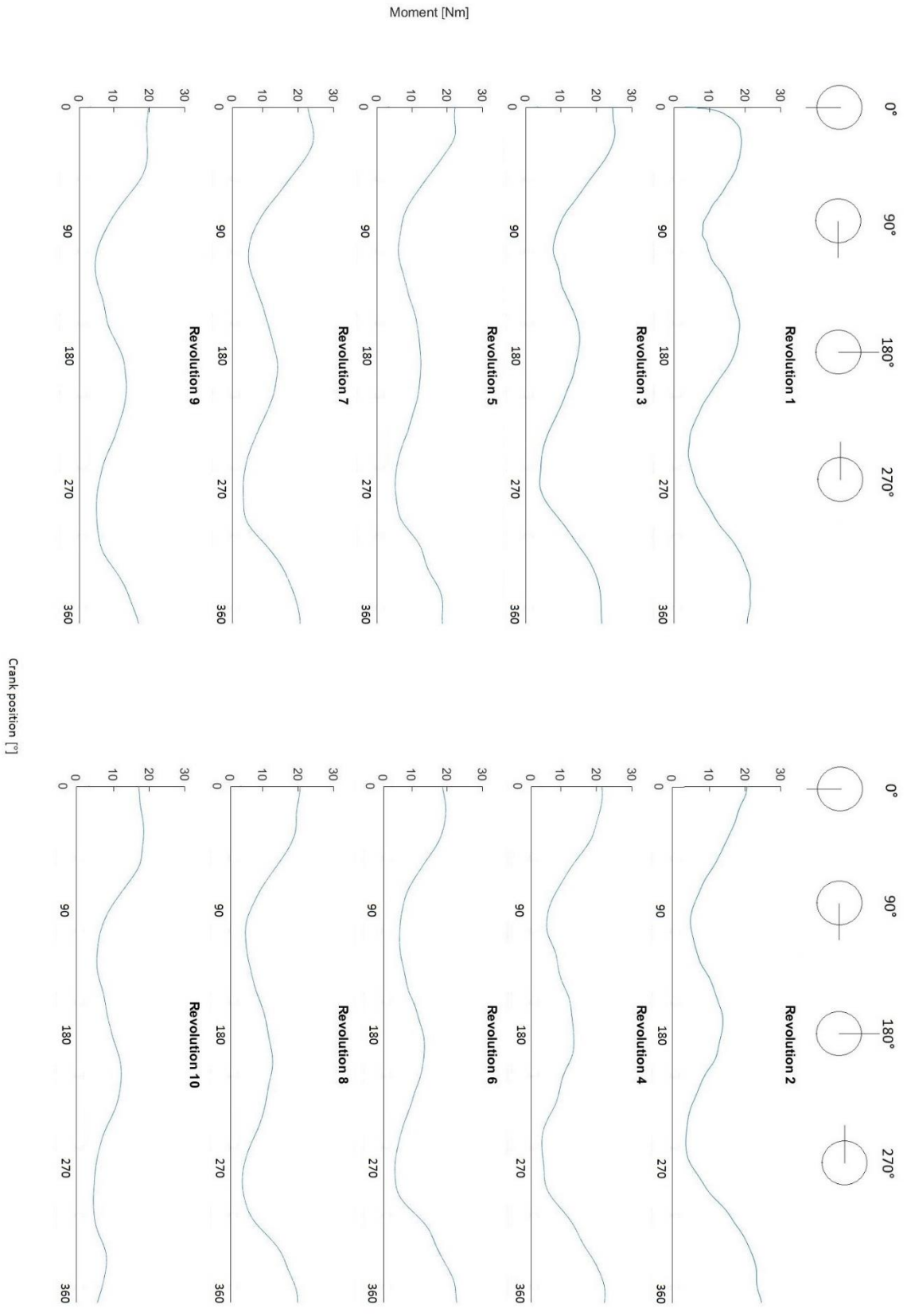

Figure 8 : Applied moment (Nm) for all ten revolutions. 0° is represents the position when the pedals are pointing vertically towards the ground.

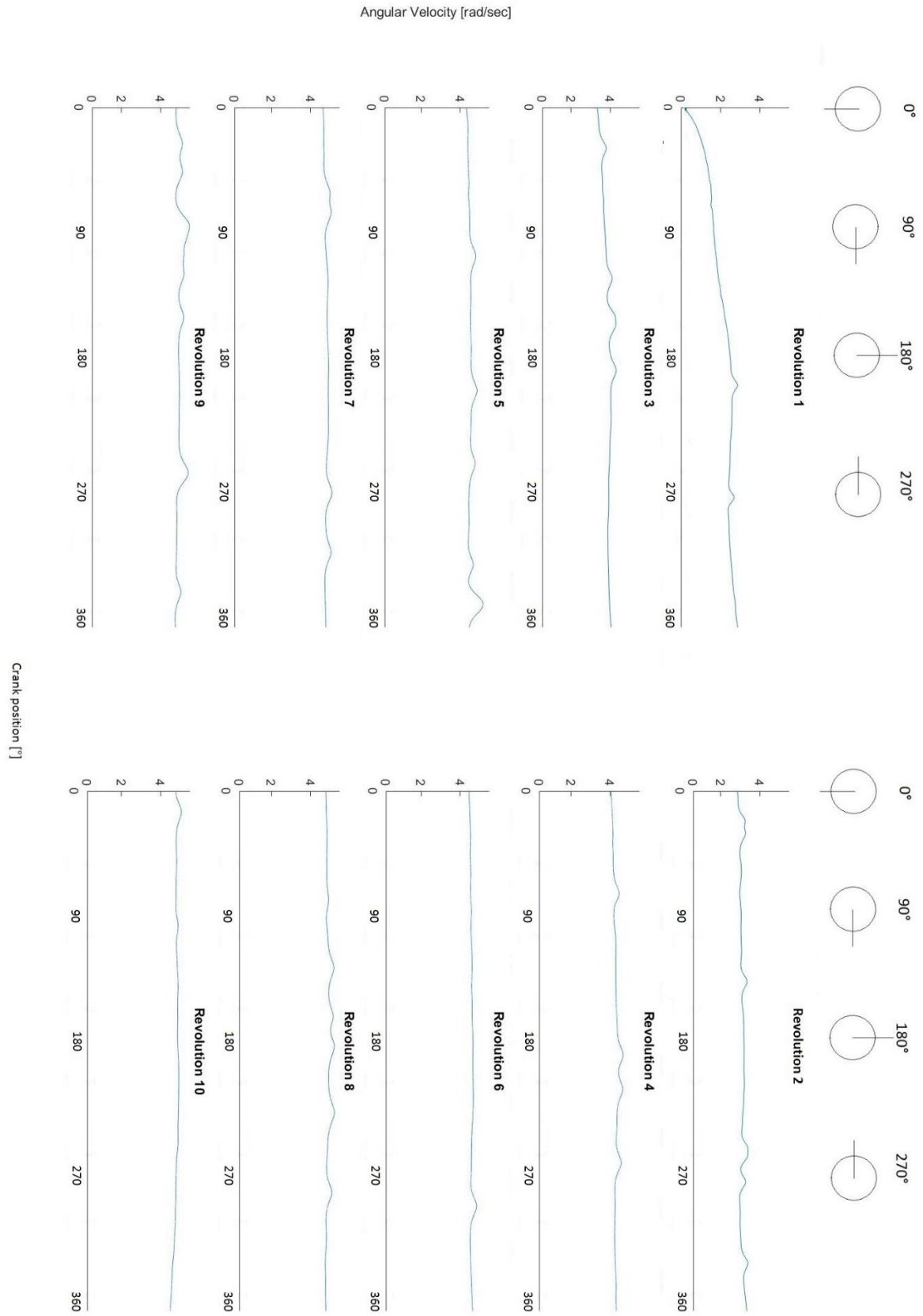

Figure 9 : Angular velocity (rad/sec) for all ten revolutions. 0° is represents the position when the pedals are pointing vertically towards the ground.

Figure 10 illustrates average power production ±SD with respect to crank position, for revolution 6-9.

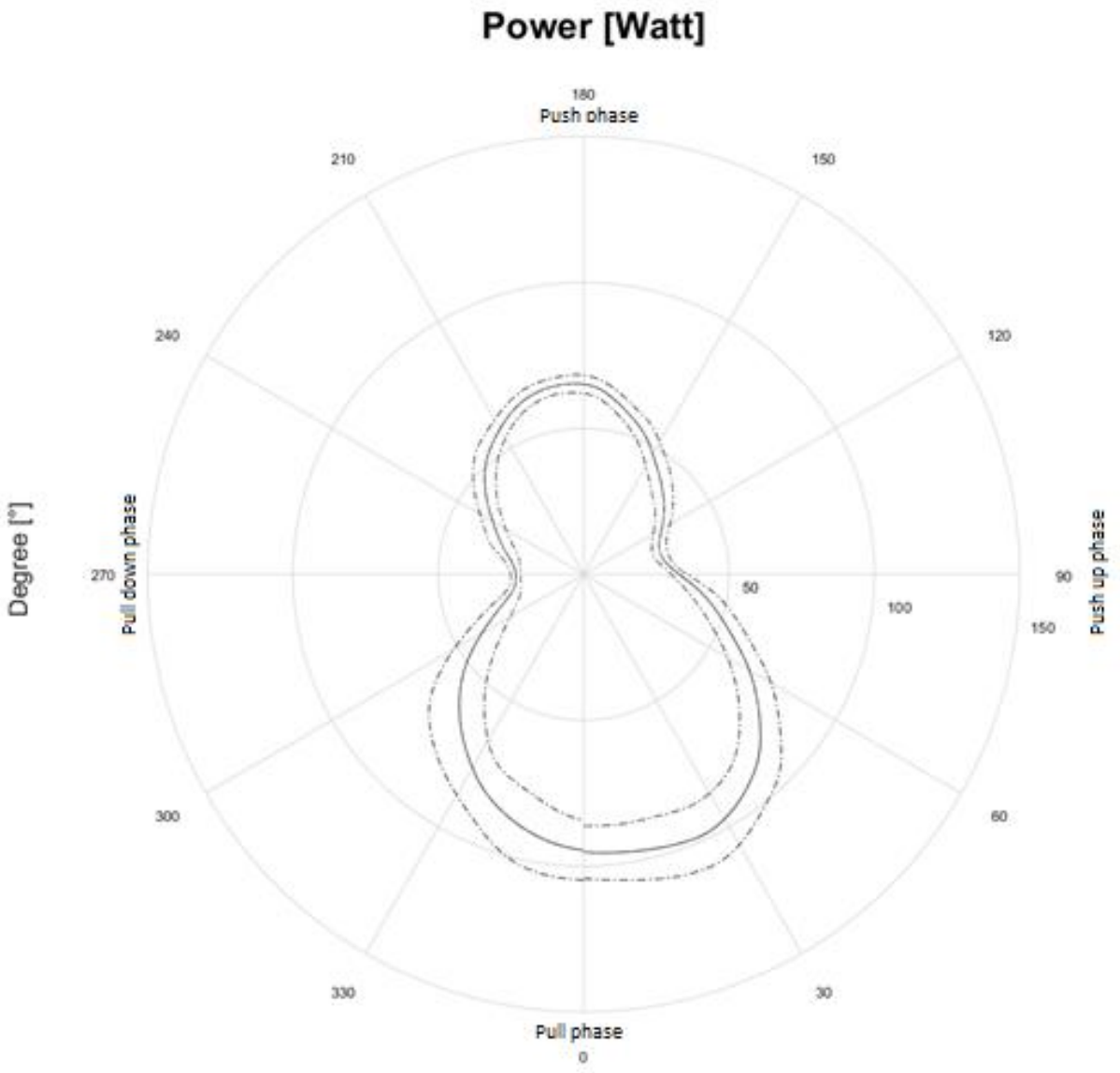

Figure 10 : Average power (watt) for revolution 6-9 (solid line) ±SD (dashed lines). 0° represents the crank start position when pedals pointing towards the ground 90° with respect to horizontal. The crank revolution is directed counter clockwise.

Discussion

The aim of this paper was to provide technical information on a wireless and relatively inexpensive force measurement system for recumbent hand cycling. The results for accuracy test showed strong coefficients of determination (R^2=1) for all three gains. The system is therefore considered valid for measuring tangential force applied to the crankshaft for different gains. The wireless delay test found 4 ms offset, thus the force measurement is slightly delayed in the synchronization with the crank position measurement. This offset was found acceptably low and therefore neglected in the synchronization. The results for angular velocity was lowest in revolution one, due to acceleration in the beginning of the propulsion. However, the velocity was close to constant for the rest of the ten revolutions, with a small velocity increase about 270° and 90°, for some of the revolutions. This suggests a small acceleration when passing the "dead points" appearing about 270° and 90° of the crank cycle.

The pattern for tangential force (figure 7) is similar to the results from the force measurement system developed by Arnet (2012a). Therefore, the system presented in this paper is considered comparable with the system developed by Arnet (2012a), with respect to measuring tangential force in hand cycling. However, the resistance on the home trainer from the initial propulsion measurement in this paper is higher, compared to the treadmill resistance used in the study by Arnet (2012a).

The present system does only measure tangential force contribution from the right arm applied to the crankshaft. Thus, it is assumed that both arms delivers the same force. In addition, the system has no measure of radial and lateral force as the system developed by Arnet (2012a). Hence, the present system does not provide the same detailed force measurement. However, the system is wireless and thereby avoids wire issues when propelling. Simultaneously, the system is applicable for field-testing and not limited to laboratory facilities.

The V-Link®-LXRS® wireless node, applied in this system, has in total seven analog channels and therefore, has the potential for connecting with seven strain gages. This enables the ability to measure force in multiple directions, such as the radial and lateral direction and thus be more comparable to the system developed by Arnet (2012a). However, the sample rate for the V-Link®-LXRS® wireless node decreases when more input sensors are connected (LORD 2015). At the same time, placement of strain gages in the optimal locations can be a difficult task. Therefore, mechanical analysis, such as Finite Element Analysis (FEA) can be performed in order to determine the areas where the greatest strain appears. In order to do so, valid boundary conditions, applied force directions and force magnitudes must be known. Further

development of this wireless system should be concerned with this purpose and so enable the opportunity to measure lateral and radial forces as well.

The participating subject in this study had no previous experience in hand cycling. Therefore, it cannot be excluded that a trained hand-biker would generate another force propulsion pattern. However, as mentioned previous, the tangential force propulsion pattern from the initial propulsion measurement in this paper, is similar to the pattern found by Arnet (2012a) who had a trained hand-biker participating in the study.

With the presented system, it is possible to perform detailed force propulsion measurement, for each crank revolution, which is not possible with currently commercially available power meters. Thus, the system has applicability potential for small handbike manufacturers, in order to undertake quantitative research experiments in the aim of optimizing handbike design.

Conclusion

This technical note introduced a wireless crank moment measurement system, which could determine tangential force and thereby moment applied to the crankshaft of a handbike. This makes it possible to analyze different crank positions (horizontal and vertical position), crank arm lengths, backrest inclination etc. with respect to optimizing propulsion force effectiveness. Futhermore, the system can provide kinetic data as input for serval biomechanical models.

Acknowledgements

The authors of this technical note would like to express our gratitude to John Hansen and Jan Stavnshøj (Department of Health Science and Technology at Aalborg University) and Søren Brunn and Klaus Kjær (Department of mechanical and manufacturing engineering at Aalborg University) for assisting the manufacturing of the present system.

References

Arnet, U. 2012a, "Development and validity of an instrumented handbike: initial results of propulsion kinetics", .

Arnet, U. 2012b, *Handcycling: a biophysical analysis*, Amsterdam: Vrije Universiteit.

Bafghi, H., A., De Haan, A., Abbasi, Horstman, A., A. & Van, D.W. 2008, "Biophysical Aspects of Submaximal Hand Cycling", *International Journal of Sports Medicine,* vol. 29, no. 8, pp. 630-638.

Bini, R.R. & Carpes, F.P.2014, *Biomechanics of Cycling / edited by Rodrigo R. Bini, Felipe P. Carpes,* Elektronisk udgave edn, Cham : Springer International Publishing.

Faupin, A. & Gorce, P. 2008, "The effects of crank adjustments on handbike propulsion: A kinematic model approach", *International Journal of Industrial Ergonomics,* vol. 38, no. 7, pp. 577-583.

Garmin *, Garmin Vector Power Meter*. Available: http://sites.garmin.com/da-DK/vector/ [2016, may].

Goosey-Tolfrey, V., Alfano, H. & Fowler, N. 2008, "The influence of crank length and cadence on mechanical efficiency in hand cycling", *European journal of applied physiology,* vol. 102, no. 2, pp. 189-194.

Hoffmann, K. 1989a, "An introduction to measurements using strain gages" in , ed. K. Hoffmann, Darmstadt : Hottinger Baldwin Messtechnik, , pp. 218.

Hoffmann, K. 1989b, "An introduction to measurements using strain gages" in , ed. K. Hoffmann, Darmstadt : Hottinger Baldwin Messtechnik, , pp. 126.

Litzenberger, S., Mally, F., & Sabo, A. 2015, "Influence of Different Seating and Crank Positions on Muscular Activity in Elite Handcycling - A Case Study", *Procedia Engineering,* vol. 112, pp. 355.

LORD, C. 2015, *, V-Link-LXRS Wireless Sensor Node User Manua*l. Available: http://files.microstrain.com/V-Link_User_Manual_(8500-0006).pdf [2016, .

Quarq *, Quarq Power meteres*. Available: http://www.quarq.com/ [2016, may].

SRM *, SRM Power meter*s. Available: http://www.srm.de/home/ [2016, may].

Verellen, J., Theisen, D. & Vanlandewijck, Y. 2004, "Influence of crank rate in hand cycling", *Medicine and science in sports and exercise,* vol. 36, no. 10, pp. 1826.

AALBORG UNIVERSITY
DENMARK

Biomechanical analysis of hand cycling propulsion movement: A musculoskeletal modelling approach

Frederik Husted Ahlers[1] & Lasse Jakobsen[2]

Abstract

Objective: Collect experimental data as input for a musculoskeletal model and Implement the data in a musculoskeletal model in order to analyse muscle activity, muscle force and joint reaction forces and moments, during recumbent hand cycling propulsion. **Method:** The kinetic measurement, obtained in this study, was done by using a customized crank moment measurement system. Two Microsoft Kinect one cameras obtained the kinematics of the hand cycling propulsion movement. The kinetics and kinematics founded the input data for a development of a musculoskeletal model, during recumbent hand cycling propulsion. **Results:** Estimation of muscle activity time and muscle force for the prime mover-muscles in the crank cycle were conducted. Simultaneously, the model estimated joint reaction forces and moments. **Discussion:** The model can be applied in studies related to performance optimization and injury prevention in relation to hand cycling.

Keywords: hand cycling, biomechanics, motion capture, musculoskeletal model**,** handbike

Introduction

Handcycling is mainly popular among paraplegics or otherwise handicapped on lower extremities for handisport (Faupin & Gorce 2008) and as a supplement to the conventional hand-rim wheelchair for transportation (Arnet 2012b). Wheelchair racing at different levels has been related to improved self-esteem and increased social activity for people with disabilities (Cooper 1990), which also has been argued to be valid for hand cycle racers (Zipfel et al. 2009). Handbikes are generally available in four different types; attachment, upright, kneeling and recumbent, dependent on whether it is meant for transport, recreational activity or for Paralympic sport competition respectively (Arnet 2012d). In this study, the focus was on the recumbent edition used for Paralympic sports competition. The recumbent bike is characterized with a low center of mass and a small frontal area, which makes it optimal for sports competition (Cooper 1990).

In relation to Paralympic sports competition, the UCI (international cycling union) has set up five hand cycling disciplines (H1-H5) determined by the athlete's injury severity (UCI). Even though the UCI has set up different competition categories, every athlete is unique with respect to disability, physics and anthropometrics, which sets demands for the hand bike manufacturers in relation to individual customization, weight reduction and interface adjustment possibilities (Zipfel et al. 2009). Therefore, the

[1] *frehust@gmail.com - M.Sc Stud. Aalborg University*
[2] *lasse@stagsted.net - M.Sc Stud. Aalborg University*

handbike interface has received interest in the scientific community (Faupin & Gorce 2008, Arnet 2012c, Litzenberger et al. 2015). Faupin & Gorce (2008) concentrated on crank position with respect to shoulder joint range of motion. Litzenberger et al. (2015) measured surface electromyography (EMG) for the major muscles, during the push phase in the handcycling propulsion cycle, at different seat angles and crank positions. The study investigated none of the major pull muscles on the back. However, the pull propulsion style has been found to be dominant during handcycling (Arnet 2012c). Therefore, the literature seems to lack a full understanding of muscle recruitment pattern for recumbent hand cycling. This can be obtained by using musculoskeletal models, able to estimate muscle activity, muscle force, joint moments and joint reaction forces, which are otherwise difficult to measure, due to invasive procedures (Skals 2015). One of the existing analytical approaches within musculoskeletal modelling is the inverse dynamic approach. Inverse dynamics calculates joint moments based on kinetic and kinematic data in order to estimate muscle activity and muscle force (Damsgaard et al. 2006).

Kinematic and kinetic data are often obtained, by using marker based motion capture systems and force transducers. Unfortunately, marker based motion capture systems and force transducers are often expensive and requires specialized laboratory facilities (Andersen 2013). Hence, research in the field of biomechanical analysis, is limited to universities and/or financially strong companies. However, recent research in the field of cheap marker-less motion capture systems has shown promising validation results (Andersen 2013, Bonnechère et al. 2014, Patrizi et al. 2016).

This leads to the aim of this study, which was two folded 1. Collect experimental input data for an inverse dynamic musculoskeletal model, during recumbent hand cycling, based on low-cost kinematic and kinetic measurements. 2. Implement the input data in a musculoskeletal model for analyzing muscle activity time, muscle force and joint reaction forces and moments. Both aims were conducted as proof-of-concept.

Method and materials

The procedure of this study consisted of two steps:

1. Collect experimental input data for an inverse dynamic musculoskeletal model.
2. Implement the input data in a musculoskeletal model for analyzing purpose.

Subject

One able-body subject (age 26, mass 82 kilograms, height 1.8 m) participated in this study. The subject had no previous experience in hand cycling. Before the experiment, the subject gave his written consent to participate in the study.

Handbike setup

A commercial available handbike was used for this experiment (Racebike model K, Wolturnus, Nibe, Denmark) and connected to KICKR bicycle home trainer (Wahoo Fitness, Atlanta, USA), mounted in a customize upside-down frame (see figure 2). The crank had a horizontal and vertical adjusting ability, which made it possible to suite a wide range of people and meet individual interface preferences. The crank was placed 370 mm vertically to the base plate of the hand bike and 130 mm horizontal with respect to the vertical tube connected to the head tube. The backrest was placed in an angle of 158° with respect to horizontal (see figure 1).

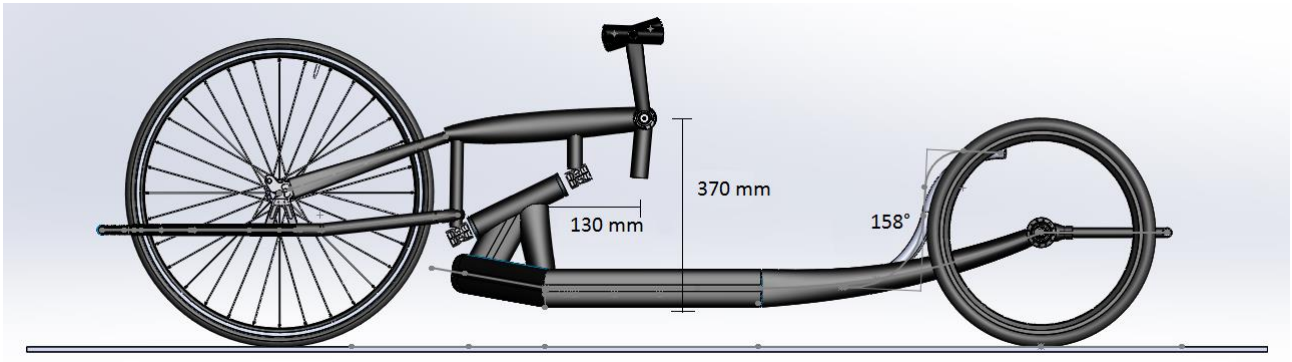

Figure 1 : Handbike setup. Measures of crank position (370 mm vertically to the base plate, 130 mm horizontal with respect to the vertical tube connected to the head tube and backrest angle of angle of 158°)

Experimental data collection

The musculoskeletal model required inputs in terms of human movement kinetic and kinematic. Kinetic is specified as the tangential force applied the crank shaft, whereas kinematic refers to the human propulsion movement.

1.1 Kinetic data collection

The kinetic measurement obtained in this study was done by using a customized force measurement system (Jakobsen & Ahlers, 2016). The force measurement was a strain gage approach and obtained applied crank moment (tangential force applied to the crankshaft). Along with the crank moment measurement, an encoder provided data for crank position and velocity (angular velocity) determination. Technical information regarding the crank moment measurement system is specified in the technical note by Jakobsen & Ahlers (2016).

1.2 Kinematic data collection

Two Microsoft Kinect one cameras (Microsoft, Seattle, USA) were used to capture the hand cycling propulsion movement. The Microsoft Kinect cameras were mounted at two custom-made camera tripods with horizontal and vertical adjusting abilities, in order to ensure optimal field of view. Two computers were running Windows 10 (Microsoft, Washington, USA) and had one USB 3 port each. Simultaneously, both computers were running iPi recorder 3.1.4.43 (iPi Soft, Moscow, Russia) and were connected as a home group via a crossed LAN-cable. Each computer was connected to one Microsoft Kinect camera. In the iPi recorder software one computer was set as master and the second as slave. Hence, the master computer triggered the recording for both Microsoft Kinect cameras simultaneously.

The recordings were processed using iPi Motion Capture Studio 3.2.6.200 (iPi Soft, Moscow, Russia). An "Actor", scaled to as the subject was manually fitted the cloud representing the subject. The Actor created simultaneously a stick figure of the subject. Subsequent, the "Refit pose" feature were applied and the "Track forward" process automatically tracked the movement. Lastly, "Jitter removal" was applied in order to improve tracking accuracy and reduce noise. The stick figure was exported as a .bvh file.

1.3 Experimental protocol

The subject propelled the handbike with a resistance of 35 %, controlled with the Bluetooth Powered Cycling and Running Workout Tracker 5.7.7 application (Wahoo Fitness, Atlanta, USA), for five minutes as warmup. Subsequently, the subject was asked to flex his elbows at 90° and simultaneously, raise his arms and keep both the upper arm and forearm parallel to the ground, with the palms facing towards the ground and hold the position for five seconds (see figure 2). This was done in order to fit the "Actor" for the subject as described in section 1.2. Next, the subject was asked to grab the handlebars and propelled the bike for 10 revolutions at 35 % with freely chosen speed.

Figure 2 : Experimental setup with handbike connected to home trainer mounted in a customize upside-down frame. The Microsoft Kinect cameras for obtaining kinematic data are located on top of the red camera tripods.

2.1 Musculoskeletal model

The Musculoskeletal model was developed in the AnyBody Modeling System v. 6.0.5 (AMS) (AnyBody Technology A/S, Aalborg, Denmark). The model was based on the *"GaitFullBody"* standard template. Muscles in the lower extremity were excluded since only the upper body extremity provides the propulsion movement in hand cycling. A constant strength muscle model independent of length and contraction velocity muscles was applied and represents the simplest conceivable muscle model (AnyBody tutorial). The model had a total of 27 degrees-of-freedom, including 2x1 DOF at the elbow joint, and 2x3 DOFs at the Glenohumeral joint. The remaining joints and degrees-of-freedom are distributed over the rest of the body, but were not considered as contributing to the propulsion movement.

Motion capture analysis in AMS is traditionally based on maker based motion capture data and cannot apply the iPi stick figure directly from the .bvh file. Hence, a translation from stick figure to marker position was required. This translation refers Andersen's et al. (2013) work and is illustrated in figure 3. The model was scaled with respect to the stick figure given from the .bvh file (figure 3). The kinematics for the model used the method of Andersen et al. (2009) and minimizes the least-square difference between markers on the model and the stick figure.

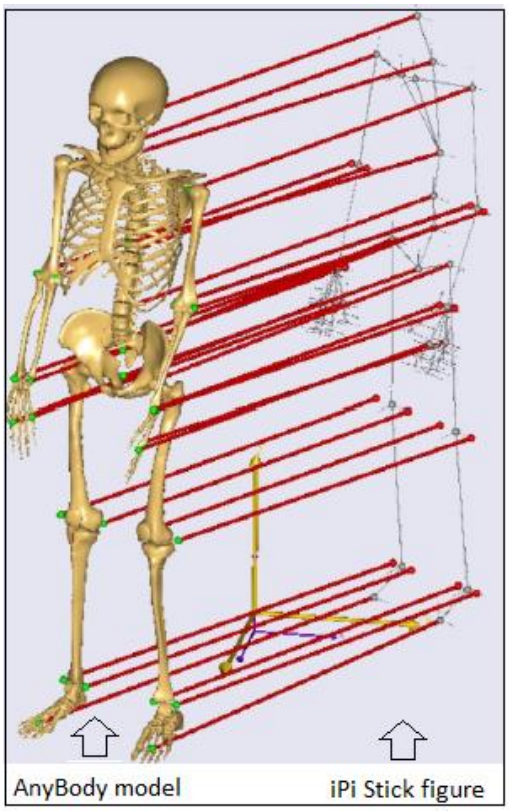

Figure 3 : Translation .BVH stick figure to marker position.

Furthermore, the model was constrained with reaction forces in the pelvic and the spine, in order to represent the boundary conditions from the seat and backrest. Additionally, the crankshaft was added as a segment, with the center of the crankshaft being X0,Y0,Z0 (center of green and red coordinate system in figure 4). Two nodes were added (X±23, Y+17, Z0 with respect to crankshaft center) (blue coordinate systems in figure 4) and represented the two handles. A revolute joint, rotating around x-axis, specified the relation between the crankshaft and the handles. The handles were bounded to the palms in the Z and Y direction.

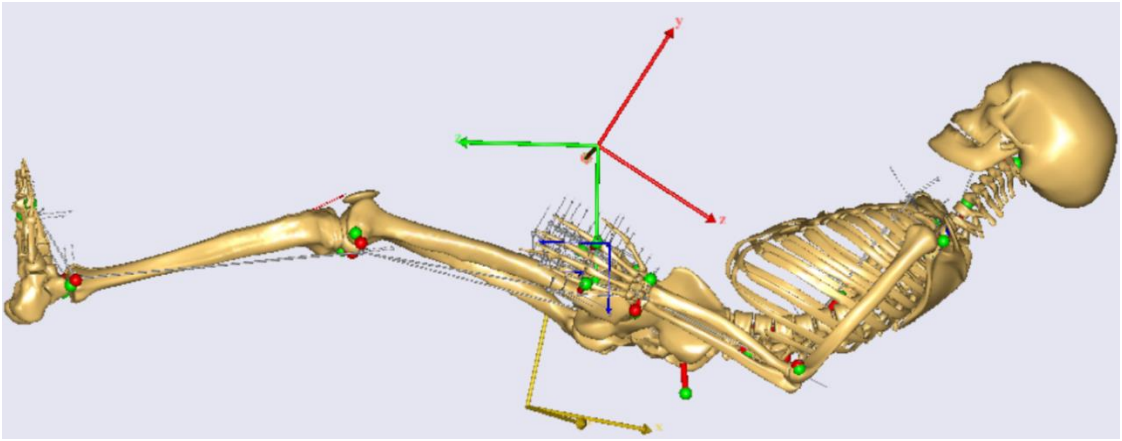

Figure 4 : AMS model of hand cycling subject. The crankshaft is illustrated as the green and red coordinate system. The blue coordinate system represents the handles.

Subsequently, an optimization study was performed with respect to the kinematics of the propulsion movement, in order to determine the crankshaft location and orientation. The revolute joint representing the crankshaft rotated about the x-axis, hence the optimization study optimized the crank position for X,Y,Z and rotation about the Z- and Y-axis.

Last, the kinetic measurement for crank moment was imported for both left and right arm. The kinetic measurement represented force contribution from the right arm and was assumed equal for both arms.

The crankshaft moment was applied as a reverse rotation force.

2.2 Data analysis

Estimated muscle force for the following muscles: Biceps, Brachialis, Latissimus Dorsi, Triceps, Pectoralis Major Thoracic, Pectoralis Major Clavicular, Deltoideus anterior, Deltoideus posterior, Infraspinatus and Supraspinatus, were exported. The muscles in the model comprised of serval subdivisions, which constitute the different directions of muscle movement. Therefore, all subdivisions for each muscles were summed in order to represent total muscle force. Furthermore, joint moments and reaction forces for the Glenohumeral joint and elbow joint were exported.

Results

All results represents the right side of the upper extremity for revolution seven. The shoulder position is located below the crank and the muscle force, joints moments and joint reaction forces reflects the position illustrated in figure 4. The pull phase was defined as 300°-60°, push up phase 60°-120°, push phase 120°-240° and the pull down phase was 240°-300°.

The kinetic measurement applied for the musculoskeletal model is presented as power (watt) in figure 5. The largest power production appears in the pull phase. The lowest power production appears in the push up phase and pull down phase, when the crank arm is placed horizontal.

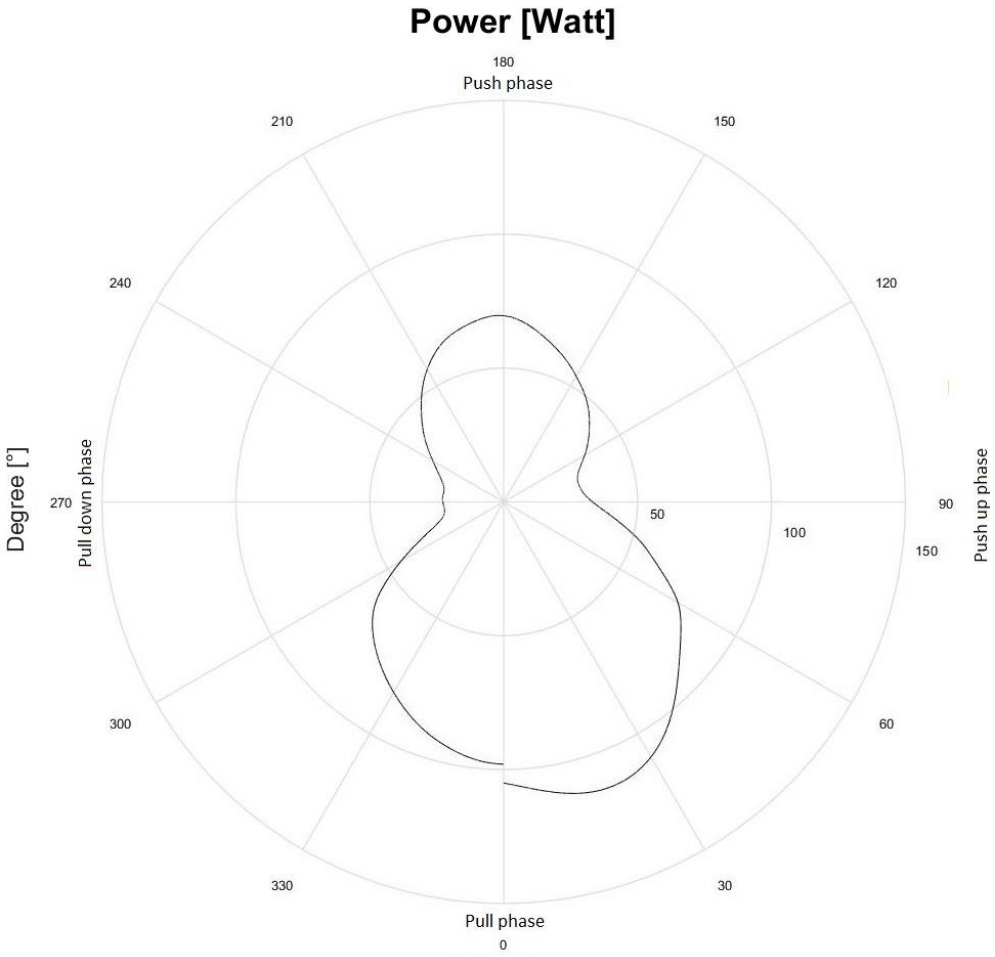

Figure 5 : Power production for revolution seven. The crank revolution is directed counter clockwise. The pull phase is defined as 300°-60°, push up phase 60°-120°, push phase 120°-240° and the pull down phase is 240°-300°.

Muscle activation times are presented in figure 6 for prime movers with respect to crank position.

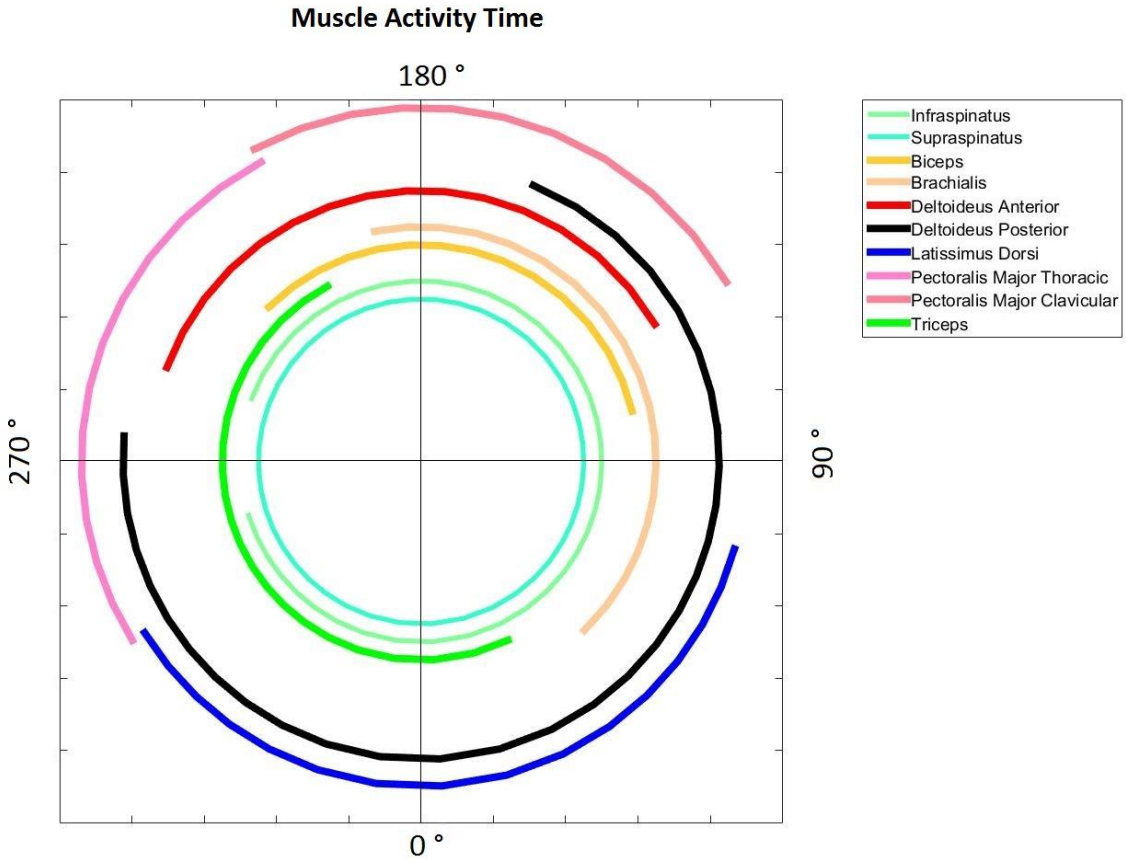

Figure 6 : Muscle activity for right side of upper extremity. Triceps (dark green), Pectoralis Major Clavicular (dark pink), Pectoralis Major Thoracic (light pink), Latissimus Dorsi (blue), Deltoideus Posterior (black), Deltoideus Anterior (red), Brachialis (light yellow), Biceps (dark yellow), Supraspinatus (turquoise) and Infraspinatus (light green), for revolution seven. The crank revolution is directed counter clockwise.

Muscle forces are presented in figure 7-8. Muscle force for the arm muscles are presented in figure 7. Triceps and Brachialis produces large force and acts as antagonists in the propulsion cycle. Muscle force for the trunk muscles are presented in figure 8. Pectoralis Major and Latissimus Dorsi acts as antagonists. However, infraspinatus produces the largest force.

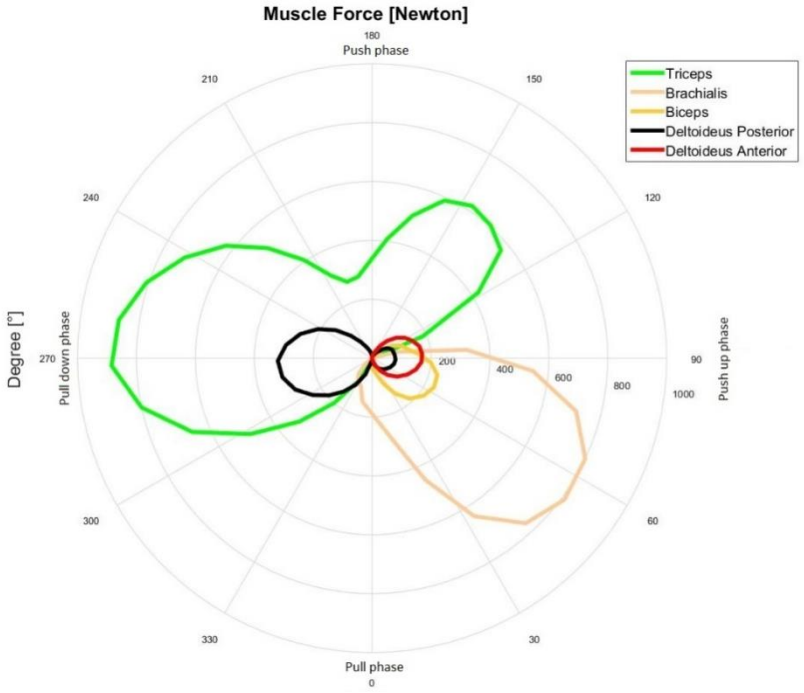

Figure 7 : Muscle force for right arm muscle. The crank revolution is directed counter clockwise.

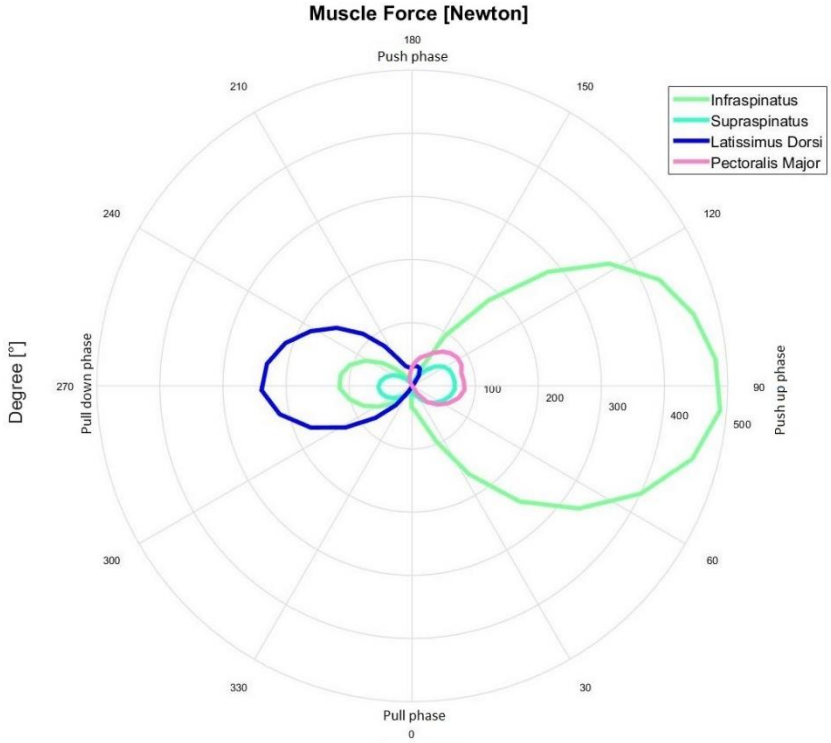

Figure 8 : Muscle force for trunk muscle. The crank revolution is directed counter clockwise.

Elbow- and Glenohumeral joint moments are illustrated in figure 9. Flexion for the Glenohumeral- and elbow joint produces the largest moment. Elbow pronation was found to contain the lowest moment.

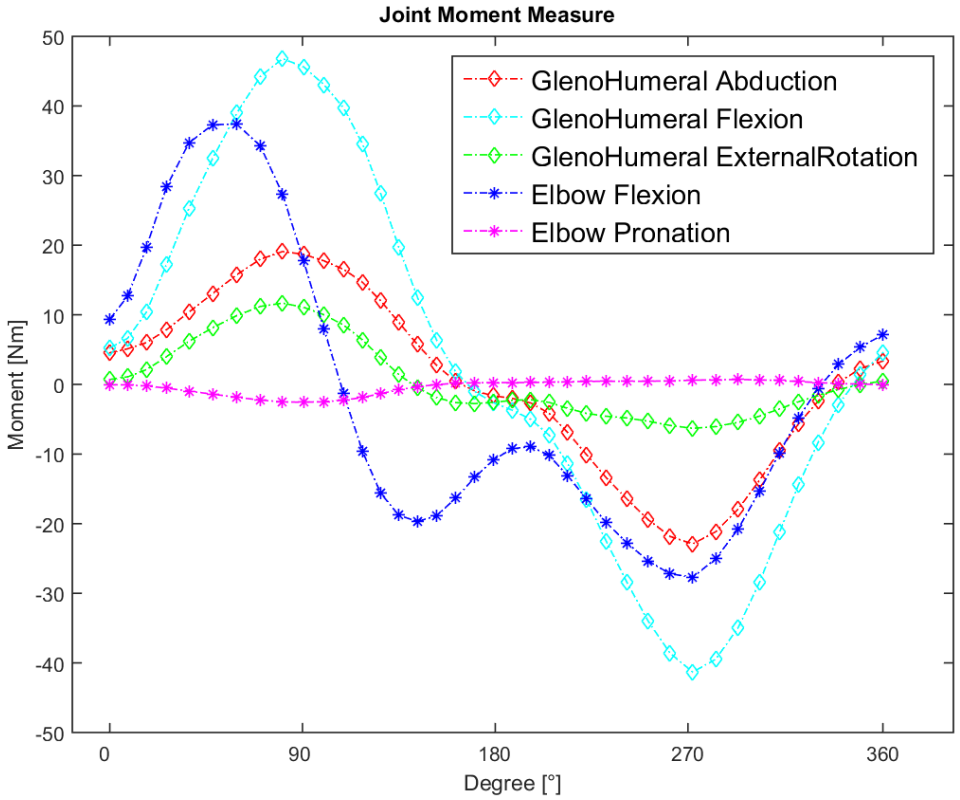

Figure 9 : Moments (Nm) for the Glenohumeral- and elbow joint with respect to crank position. 0° represents the crank start position when pedals pointing towards the ground 90° with respect to horizontal.

Reaction forces for the Glenohumeral joint appears in figure 10. All the forces seem to peak around 90° and 270°, when the crank arms are horizontally located.

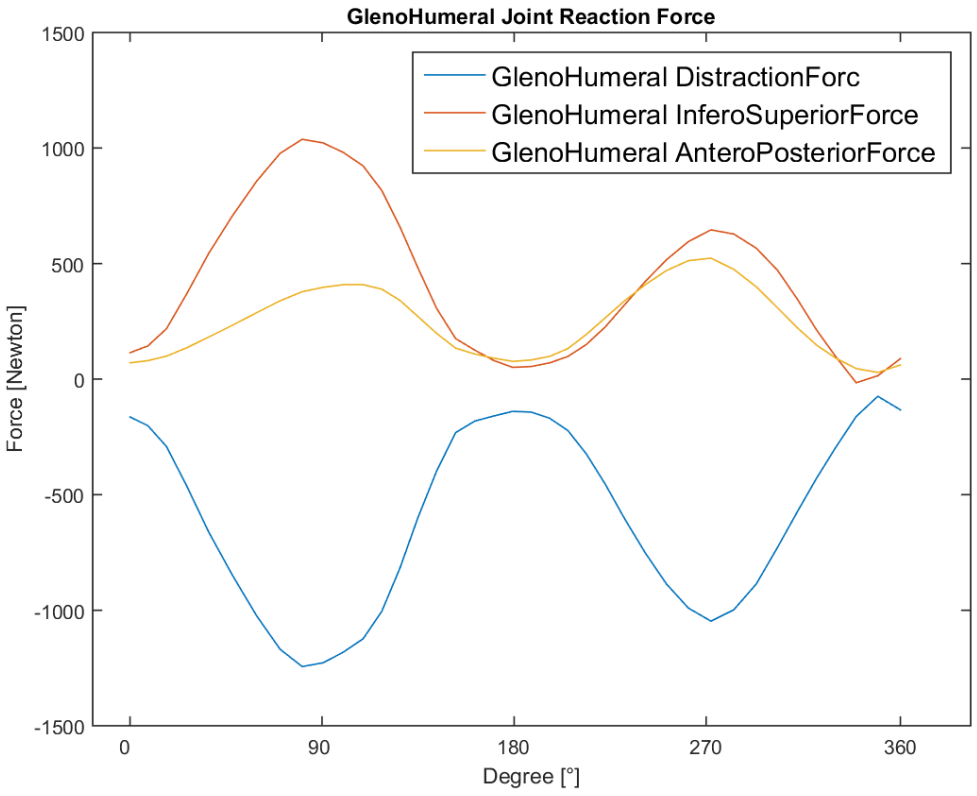

Figure 10 : Glenohumeral joint reaction force with respect to crank position. 0° represents the crank start position when pedals pointing towards the ground 90° with respect to horizontal.

Discussion

The pull phase in the propulsion cycle was found to be dominant for power production (see figure 5). This is in accordance with previous findings for submaximal hand cycling propulsion (Arnet 2012c). The results for joint moments (figure 9) illustrates a higher flexion moment for the Glenohumeral joint compared to the elbow joint. Joint moment are produced by muscles working across the joint, which suggest higher demands for the muscles working across the Glenohumeral joint compared to the muscles working across the elbow joint. This is in correlation with the relatively high muscle force found for Triceps, working as agonist to Latissimus Dorsi (see figure 7 and 8) for extension of the Glenohumeral joint in approximately 270° of the crank cycle. Muscle force for Infraspinatus reaches peak force in approximately 90° of the crank cycle and is properly due to eccentric muscle work in order to stabilize the Glenohumeral joint. The muscle activation time shown in figure 6 is similar to the muscle activation time found with EMG measurement by Litzenberger et al. (2015) for triceps and biceps. Pectoralis Major in this study is active prior in the crank cycle compared to Pectoralis Major in the study by Litzenberger et al. (2015). Deltoideus in this study is divided into an anterior and posterior part and is therefore difficult to compare with Deltoideus activation in the study by Litzenberger et al. (2015), since the anterior/posterior positioning of the EMG electrode is not specified. Litzenberger et al. (2015) had no measure for Latissimus Dorsi, which therefore cannot be compared. In addition, the muscle activation time for infraspinatus and supraspinatus presented in this study is difficult to measure with EMG, due to in vivo placement of the electrodes. The limitations of EMG measurements makes musculoskeletal model prediction of muscle activity and joint reaction force valuable. The Glenohumeral distraction force reaches 1243 N and 1047 N in the pull down and push up phase respectively. The Glenohumeral distraction force has been acknowledge as a risk factor for developing of shoulder injuries (Stuelcken et al. 2010, Werner et al. 2006). Therefore, minimization of the Glenohumeral distraction force potentially minimize the injury risk in hand cycling. However, the Glenohumeral distraction force, found in this study for hand cycling, is more than twice as high compared to explosive cricket fast bowling movement (Stuelcken et al. 2010). Therefore, the results for Glenohumeral distraction force found in this study must be interpreted with caution.

A challenge arises in the AnyBody model segment scaling, when applied paraplegics or lower limb amputees due to abnormal body mass proportions. The model scales body segments with respect to total body mass, which for paraplegics or lower limb amputees can be a poor assumption, due to significant reduced muscle size or leg absence. Thus, the models assumed maximum muscle strength in the upper extremity could be lower, compared to reality. Therefore, muscle activity, which is a percentage of

maximum muscle activity, may be a poor measure for this musculoskeletal model, when applied paraplegics. Instead, muscle force is recommended as measure for muscle work.

The Microsoft Kinect cameras applied in this study as motion capture system is a low-cost solution compared to traditional marker based motion capture systems. Therefore, the kinematic quality of the Kinect cameras can be expected to be of minor quality, compared to high-end marker based motion capture system. A study validated the Microsoft Kinect 360 camera (first version) with a marker based system and found good correlation for shoulder abduction, but less accuracy for elbow flexion and lower extremity movements (Bonnechère et al. 2014). However, the Microsoft Kinect one camera used in this study, has underwent serval improvements compared to Microsoft Kinect 360, including five additional joint determinations in the upper body for improved tracking accuracy (Microsoft corporation. 2016). Further studies in relation to Microsoft Kinect one camera validation must clarify the exact accuracy.

This study presents a model able to predict muscle activity time, muscle force, joint reaction forces and joint moments, for the propulsion cycle, during recumbent hand cycling. This musculoskeletal model approach and results provides the base for study opportunities related to interface setup, in order to minimize injury risk. E.g. for calculation of Glenohumeral contact force, which previously has been found to be an injury risk for wheelchair handrim propulsion and hand cycling (Arnet 2012a). Furthermore, the model can be applied in studies related to performance optimization, aimed to lowering muscle activity or enhance force production for selected muscles, by changing the handbike interface setup. Research in the aforementioned fields can provide handbike design guidelines for handbike manufactures, whether suited for minimizing injury risk or performance enhancement.

Conclusion

This study presented a human musculoskeletal model during hand cycling propulsion in a recumbent handbike. The model was able to predict muscle activity time, muscle force, joint moments and joint reaction forces. Furthermore, this study presented a novel and low cost method for obtaining kinematic and kinetic data as input for the musculoskeletal model. Due to the low cost method for obtaining kinematic and kinetic data, this study suggested a research opportunity for handbike designers and manufactures.

Acknowledgements

The authors of this study expresses gratitude to Michael Skipper Andersen for assisting the setup of the musculoskeletal model. Furthermore, we addresses our gratitude to Wolturnus A/S for providing the handbike used in this study.

References

Andersen, M.S., Damsgaard, M. & Rasmussen, J. 2009, "Kinematic analysis of over- determinate biomechanical systems", *Computer methods in biomechanics and biomedical engineering,* vol. 12, no. 4, pp. 371-384.

Andersen, M.S. 2013, "Full-body musculoskeletal modeling using dual microsoft kinect sensors and the anybody modeling system", , pp. 23-24.

AnyBody, T.A. *AnyBody tutorial - muscle modeling - lesson 5*, AnyBody Modeling System v. 6.0.5 edn.

Arnet, U. 2012a, *Handcycling: a biophysical analysis Chapter 4*, Amsterdam: Vrije Universiteit.

Arnet, U. 2012b, *Handcycling: a biophysical analysis Chapter 5*, Amsterdam: Vrije Universiteit.

Arnet, U. 2012c, *Handcycling: a biophysical analysis Chapter 6*, Amsterdam: Vrije Universiteit.

Arnet, U. 2012d, *Handcycling: a biophysical analysis Chapter 7*, Amsterdam: Vrije Universiteit.

Bonnechère, B., Jansen, B., Salvia, P., Bouzahouene, H., Omelina, L., Moiseev, F., Sholukha, V., Cornelis, J., Rooze, M. & Van, S.J. 2014, "Validity and reliability of the Kinect within functional assessment activities: Comparison with standard stereophotogrammetry", *Gait & posture,* vol. 39, no. 1, pp. 593-598.

Cooper, R.A. 1990, "Wheelchair racing sports science: a review", *Journal of rehabilitation research and development,* vol. 27, no. 3, pp. 295.

Damsgaard, M., Rasmussen, J., Christensen, S., Surma, E. & de Zee, M. 2006, "Analysis of musculoskeletal systems in the AnyBody Modeling System", *Simulation Modelling Practice and Theory,* vol. 14, no. 8, pp. 1100-1111.

Faupin, A. & Gorce, P. 2008, "The effects of crank adjustments on handbike propulsion: A kinematic model approach", *International Journal of Industrial Ergonomics,* vol. 38, no. 7, pp. 577-583.

Jakobsen, Lasse & Ahlers, Frederik Unpublished technical note 2016, "Development of a wireless crank moment measurement-system for handbike: Initial results of propulsion kinetics".

Litzenberger, S., Mally, F., & Sabo, A. 2015, "Influence of Different Seating and Crank Positions on Muscular Activity in Elite Handcycling - A Case Study", *Procedia Engineering,* vol. 112, pp. 355.

Microsoft, corporation. 2016 , *Kinect hardware*. Available: https://developer.microsoft.com/en-us/windows/kinect/hardware.

Patrizi, A., Pennestrì, E. & Valentini, P.P. 2016, "Comparison between low- cost marker- less and high- end marker- based motion capture systems for the computer- aided assessment of working ergonomics", *Ergonomics,* vol. 59, no. 1, pp. 155-162.

Skals, S.L. 2015, *Prediction of ground reaction forces and moments during sports-related movements*.

Stuelcken, C.M., Ferdinands, R.E.D., Ginn, K.A. & Sinclair, J.P. 2010, "The Shoulder Distraction Force in Cricket Fast Bowling", *Journal of Applied Biomechanics,* vol. 26, pp. 373.

UCI *UCI cycling regulations*
Part 16 para-cycling
(version on 1.02.14), http://www.uci.ch/mm/Document/News/Rulesandregulation/16/26/73/16han-E_English.PDF.

Werner, S.L., Jones, D.G., Guido,John A., Jr, & Brunet, M.E. 2006, "Kinematics and kinetics of elite windmill softball pitching", *The American Journal of Sports Medicine,* vol. 34, no. 4, pp. 597.

Zipfel, E., Olson, J., Puhlman, J. & Cooper, R.A. 2009, "Design of a custom racing hand- cycle: Review and analysis", *Disability & Rehabilitation: Assistive Technology, 2009,* vol. 4; Vol.4, no. 2; 2, pp. 119; 119-128; 128.